

# Unbalanced penalization: A new approach to encode inequality constraints of combinatorial problems for quantum optimization algorithms

J. A. Montañez-Barrera,<sup>1,\*</sup> A. Maldonado-Romo,<sup>2,3</sup> Dennis Willsch,<sup>1</sup> and Kristel Michielsens<sup>1,4,5</sup>

<sup>1</sup>*Institute for Advanced Simulation, Jülich Supercomputing Centre,  
Forschungszentrum Jülich, 52425 Jülich, Germany*

<sup>2</sup>*Centro de investigación en Computación, Instituto Politécnico Nacional, México*

<sup>3</sup>*Entropica Labs, 186b Telok Ayer Street, Singapore 068632*

<sup>4</sup>*AIDAS, 52425 Jülich, Germany*

<sup>5</sup>*RWTH Aachen University, 52056 Aachen, Germany*

Solving combinatorial optimization problems of the kind that can be codified by quadratic unconstrained binary optimization (QUBO) is a promising application of quantum computation. Some problems of this class suitable for practical applications such as the traveling salesman problem (TSP), the bin packing problem (BPP), or the knapsack problem (KP) have inequality constraints that require a particular cost function encoding. The common approach is the use of slack variables to represent the inequality constraints in the cost function. However, the use of slack variables increases considerably the number of qubits and operations required to solve these problems using quantum devices. In this work, we present an alternative method that does not require extra slack variables and consists of using an unbalanced penalization function to represent the inequality constraints in the QUBO. This function is characterized by having a larger penalization when the inequality constraint is not achieved than when it is. We tested our approach for the TSP, the BPP, and the KP. For all of them, we are able to encode the optimal solution in the vicinity of the cost Hamiltonian ground state. This new approach can be used to solve combinatorial problems with inequality constraints with a reduced number of resources compared to the slack variables approach using quantum annealing or variational quantum algorithms.

**Keywords:** QUBO; inequality constraints; knapsack; bin packing; travel salesman problem; quantum optimization; VQA; QAOA; quantum annealing; combinatorial optimization.

## I. INTRODUCTION

The exploration of quantum enhancement in combinatorial optimization problems has been extended over several years. There are three main reasons for this; first, many combinatorial optimization problems can be encoded in Hamiltonians, the ground state being the optimal solution of the problem [1, 2]; second, they are commonly hard to solve and have practical applications [3]; and third, the quantum algorithms to solve these problems need few resources and can be tested on current state-of-the-art quantum hardware [4, 5].

The usual approach for encoding combinatorial optimization problems on quantum processing units (QPUs) is to transform them in their quadratic unconstrained binary optimization (QUBO) representation and obtain the cost Hamiltonian after a change of variables. In the QUBO encoding, the constraints of the combinatorial optimization problems are added to the cost function as penalization terms along with the objective function.

However, we are currently in a noisy intermediate-scale quantum (NISQ) stage and QPUs are restricted in terms of qubits number and circuit depth [6]. The main consequence is that numerous problems solvable by quantum

algorithms such as Shor’s algorithm [7, 8] remain impractical to test on real quantum hardware. Despite the fact, solving combinatorial optimization problems is possible on current hardware. For example, on gate-base QPUs, Variational Quantum Algorithms (VQA) [9] thanks to their short depth and resistance to noise are applicable even with the above limitations [10]. Besides, quantum annealers, using the quantum annealing (QA) principle, are another quantum technology used to solve combinatorial optimization problems [11, 12]. In this respect, QA shows some advantages under certain conditions compared to classical annealing [13–15].

Of the aforementioned VQA algorithms, the most studied for combinatorial optimization problems is the Quantum Approximate Optimization algorithm (QAOA) [16]. Even if it is still unclear whether QAOA will give any advantage compared with classical algorithms, its simplicity makes it of great interest for analytical and practical purposes [4]. In the simplest QAOA version, the cost Hamiltonian of a combinatorial optimization problem is encoded in a parametric unitary gate along with a “mixer”, a second parametric unitary gate that does not commute with the first unitary gate. In this context, the parameters are adjusted to minimize the cost Hamiltonian expectation value using a classical optimizer. Multiple approaches for solving combinatorial optimization problems using QAOA or QA can be found in the literature, for example, in logistics [17], finance [5, 18–20], energy [21], communications [22], automotive industry

---

\* Corresponding author: J. A. Montañez-Barrera; j.montanez-barrera@fz-juelich.de

[23], traffic signal [24], among others.

From the different sets of problems that can be solved using quantum hardware, the ones with inequality constraints required an extra number of variables to get their QUBO representation. For example, the BPP and the TSP have many inequality constraints that increase with the number of items and cities, respectively. The usual approach implemented in SDKs such as Qiskit or D-wave Ocean is to use slack variables to encode the inequality constraints. Still, such an approach increments the number of qubits and connections needed to solve these problems.

In this paper, we propose an alternative method to encode inequality constraints in the QUBO formulation of combinatorial optimization problems. In this new heuristic encoding method, inequality constraints are encoded using an unbalanced penalization formula. This formulation adds larger penalization when the inequality constraint is not fulfilled than when it is. We test our method using OpenQAOA [25] a python based library developed by Entropica Labs on the TSP, the BPP, and the KP. In the majority of the cases the optimal solution is encoded in the ground state. However, in some cases, the optimal solution is in the vicinity of the ground state. For such cases, our method still provides a good approximation given the whole set of eigenvalues.

The rest of the paper is organized as follows. Sec. II provides a description of the combinatorial optimization problems implementation using QUBOs and an overview of the TSP, BPP, and KP, while Section III presents a description of the *unbalanced penalization* approach and a new metric called coefficient of performance (CoP) to study the efficiency of QAOA to solve combinatorial optimization problems. Section IV presents the results and discussion. Finally, Section V provides some conclusions. The source code for the new method setup and implementation on the TSP, BPP, and KP can be found at <https://jugit.fz-juelich.de/qip/unbalanced-penalizations-qubo>.

## II. QUADRATIC UNCONSTRAINED BINARY OPTIMIZATION

The set of combinatorial problems that can be represented by the QUBO formulation are characterized by functions of the form

$$f(x) = \frac{1}{2} \sum_{i=1}^n \sum_{j=1}^n q_{ij} x_i x_j, \quad (1)$$

where  $n$  is the number of variables,  $q_{ij} \in \mathbb{R}$  are coefficients associated to the specific problem, and  $x_i \in \{0, 1\}$  are the binary variables of the problem. Note that  $x_i x_i \equiv x_i$  and  $q_{ji} = q_{ji}$  in this formulation. Therefore,

the general form of a combinatorial optimization problem solvable by QPUs is given by the cost function

$$f(x) = \sum_{i=1}^{n-1} \sum_{j>i}^n q_{ij} x_i x_j + \sum_{i=1}^n q_{ii} x_i, \quad (2)$$

and equality constraints given by

$$\sum_{i=1}^n c_i x_i = C, \quad c_i \in \mathbb{R} \quad (3)$$

and inequality constraints given by

$$\sum_{i=1}^n l_i x_i \geq B, \quad l_i \in \mathbb{R}. \quad (4)$$

To transform these problems into the QUBO formulation the constraints are added as penalization terms. In this respect, the equality constraints are included in the cost function using the following penalization term

$$\lambda_0 \left( \sum_{i=1}^n c_i x_i - C \right)^2 \quad (5)$$

where  $\lambda_0$  is a penalization coefficient that should be chosen to guarantee that the equality constraint is fulfilled. In the inequality constraint case, the common approach is to use a slack variable [26, 27]. The slack variable is an auxiliary variable that makes a penalization term vanish when the inequality constraint is achieved,

$$\sum_{i=1}^n l_i x_i + \text{slack} - B = 0. \quad (6)$$

Therefore, when Eq. (4) is satisfied, Eq. (6) is 0. This means the slack variable must be in the range  $0 \leq \text{slack} \leq \max_x \sum_{i=1}^n l_i x_i - B$ . To represent the *slack* variable in binary form, the slack is decomposed in  $N = \lceil \log_2(\max_x \sum_{i=1}^n l_i x_i - B) \rceil$  binary variables:

$$\text{slack} = \sum_{k=1}^N 2^k s_k \quad (7)$$

where  $s_k$  are the slack binary variables. Then, the inequality constraints are added as penalization terms by

$$\lambda_1 \left( \sum_{i=1}^n l_i x_i + \sum_{k=1}^N 2^k s_k - B \right)^2. \quad (8)$$

Combining Eq. (2) and the two kinds of constraints Eq. (5) and Eq. (8), the general QUBO representation of a given combinatorial optimization problem is given by

$$\min_x \left( \sum_{i=1}^{n-1} \sum_{j>i}^n c_{ij} x_i x_j + \sum_{i=1}^n h_i x_i + \lambda_0 \left( \sum_{i=1}^n q_i x_i - C \right)^2 + \lambda_1 \left( \sum_{i=1}^n l_i x_i + \sum_{k=1}^N 2^k s_k - B \right)^2 \right). \quad (9)$$

Note that after some manipulations, Eq. (9) can be rewritten in the Eq. (2) form. The last step to represent the QUBO problem on QPUs is to change the  $x_i$  variables by spin variables  $z_i \in \{1, -1\}$ . This is the general idea of the cost Hamiltonian model and means that  $x_i = (1 - z_i)/2$ . Hence, the Eq. (2) represented by the cost Hamiltonian model is given by

$$H_c(z) = \sum_{i=1}^{n-1} \sum_{j>i}^n q_{ij} (1 - z_i)(1 - z_j)/4 + \sum_{i=1}^n q_{ii} (1 - z_i)/2. \quad (10)$$

### A. Traveling salesman problem

In the TSP, a traveler has to stop by a set of cities, the problem is to find the shortest route to visit every city once and return to the initial point. Different formulations of the TSP exist, but in this work, we focus on the Dantzig-Fulkerson-Johnson (DFJ) formulation [28] which is a solid formulation for avoiding sub-tours in the solution. Note that even though there are other formulations of this problem that do not require inequality constraints for a fully connected graph, e.g., [1]. The DFJ formulation can be generalized to a non-fully connected graph and to the vehicle routing problem (VRP), but more importantly, it is used here to test the capabilities of the unbalanced penalization method to encode multiple inequality constraints. In this formulation, the problem is given by

$$\min \sum_{i=1}^{n-1} \sum_{j>i}^n c_{ij} x_{ij}, \quad (11)$$

subject to the set of constraints,

$$\sum_{i=1, i \neq j}^n x_{ij} = 1 \quad j = 1, \dots, n, \quad (12)$$

$$\sum_{j=1, j \neq i}^n x_{ij} = 1 \quad i = 1, \dots, n, \quad (13)$$

$$\sum_{i \in Q} \sum_{j \neq i, j \in Q} x_{ij} \leq |Q| - 1 \quad \forall Q \subseteq \{1, \dots, n\}, |Q| \geq 2 \quad (14)$$

where  $n$  is the number of cities,  $c_{ij}$  is the distance between the cities  $i$  and  $j$ ,  $x_{ij}$  is a binary variable that represents if the path from the city  $i$  to the city  $j$  is used or not, and  $Q$  represents a sub-tour on a set of cities. From the above equations, Eq. (11) is the cost function

for the distance traveled, Eq. (12) and Eq. (13) restrict the traveler to take only one path to come in and one to come out of a city, and Eq. (14) are the inequality constraints that prohibit sub-tours in the solution. Of all the inequality constraints analyzed in this work, constraint 14 is the most expensive in terms of the number of slack variables. Fig. 1 a) shows the number of qubits needed to represent the TSP for a different number of cities.

For this work, we place random cities on a 50x50 grid with the values  $c_{ij}$  as the Euclidian distance between cities. We vary from 2 to 7 cities and for problems up to 5 cities, we generate 10 random problems to test the generalization of our method.

### B. Bin packing problem

In the BPP, a collection of items must be stored in the minimum possible number of bins. In this case, the items have a weight associated and the bins are restricted to carry a maximum weight. This problem has many real applications in areas such as loading trucks with a weight restriction [29], container scheduling [30], or design of FPGA chips [31]. In terms of complexity, the BPP is an NP-hard problem and its formulation is given by

$$\min \sum_{j=1}^m y_j, \quad (15)$$

subject to:

$$\sum_{i=1}^n s_i x_{ij} \leq B y_j \quad \forall j = 1, \dots, m, \quad (16)$$

$$\sum_{j=1}^m x_{ij} = 1 \quad \forall i = 1, \dots, n, \quad (17)$$

$$x_{ij} \in \{0, 1\} \quad \forall i = 1, \dots, n \quad j = 1, \dots, m, \quad (18)$$

$$y_j \in \{0, 1\} \quad \forall j = 1, \dots, m, \quad (19)$$

where  $n$  is the number of items,  $m$  is the number of bins,  $s_i$  is the  $i$ -th item weight,  $B$  is the maximum weight of each bin,  $x_{ij}$  and  $y_j$  are binary variables that represent if the item  $i$  is in the bin  $j$ , and whether bin  $j$  is used or not, respectively. From the above equations, Eq. (15) is the cost function to minimize the number of bins, Eq. (16) is the inequality constraint for the maximum weight of a bin, Eq. (17) is the equality constraint to restrict that an item is only in one of the bins, and 18 and 19 means that  $y_i$  and  $x_{ij}$  are binary variables.

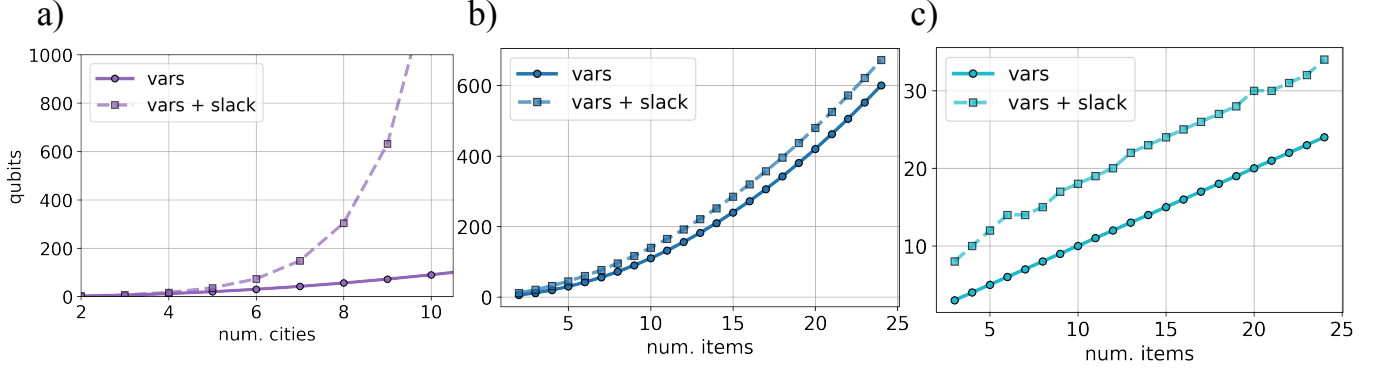


FIG. 1. Number of qubits needed to solve a) the TSP for different number of cities, b) the BPP for different number of items, and c) the KP for different number of items. The solid line represents the number of variables of the problem and the dashed line represent the variables of the problem plus the slack variables needed to represent the inequality constraints of the problem for a different number of nodes.

Fig. 1 b) shows the number of variables needed to solve the BPP when the number of bins is equal to the number of items. The weights are chosen randomly with values between 4 and 20 and the maximum bin weight equal to 20. The solid line represents the number of qubits needed for a specific number of items in the BPP and the dashed line represents the same BPP but with the slack variables encoding. Without losing generality, two further simplifications are made, the first assigns the first item to the first bin  $x_{11} = 1$  and therefore  $x_{1j} = 0 \forall j \in \{2, \dots, m\}$ . In the second simplification, because the minimum number of bins required is known, we can replace  $y_j = 1 \forall j \in \{1, 2, \dots, N_{min}^{bin}\}$  with  $N_{min}^{bin} = \lceil (\sum_{i=1}^n s(i)) / B \rceil$ .

### C. Knapsack problem

In the KP, a set of items with associated weights and values should be store in a knapsack. The problem is to maximize the value of the items transported in the knapsack. The KP is restricted by the maximum weight the knapsack can carry. The KP is the simplest nontrivial integer programming model with binary variables, only one constraint, and positive coefficients. It is formally defined by

$$\max \sum_{i=1}^n p_i x_i, \quad (20)$$

$$\sum_{i=1}^n w_i x_i \leq W, \quad (21)$$

where  $n$  is the number of items,  $p_i$  and  $w_i$  is the value and weight of the  $i$ th item, respectively,  $x_i$  is the binary variable that represents whether the  $i$ th item is in the knapsack or not, and  $W$  is the maximum weight that the knapsack can transport. Fig. 1 c) shows the number of qubits needed to solve the KP for a different number

of items. The solid line is the number of qubits needed to represent the problem and the dashed line is the corresponding number of variables needed to represent the problem using the slack variables encoding approach. In this case, the set of problems is created with weights and values selected randomly for values ranging between 1 and 63, weights between 1 and 127, and knapsack maximum weight equal to 70% of the sum of the weights of all the items.

An estimate of the number of slack variables needed to represent the QUBO of the TSP, the BPP, and the KP is shown in Fig. 2. In the TSP, the number of slack variables increases exponentially with the number of cities added. In the BPP, it requires many slack binary variables increasing proportionally to the number of bins of the problem. Lastly, in the KP, the number of slack variables needed is constant and depends on the maximum weight allowed in the knapsack.

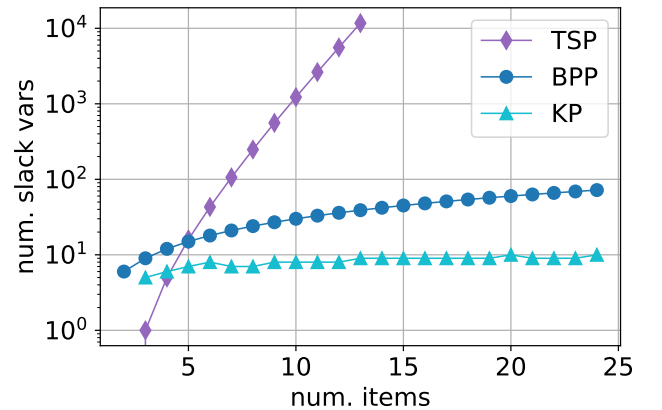


FIG. 2. The number of slack variables needed to solve the TSP, the BPP, and the KP based on the number of items for the BPP and the KP and cities for the TSP (the solid lines are guiding lines).

### III. UNBALANCED PENALIZATION

The unbalanced penalization approach we propose is an approximation for including inequality constraints of combinatorial optimization problem in the QUBO representation of the cost function. This method does not require additional slack variables, and the inequality constraint of Eq. (4) given by

$$h(x) = \sum_i l_i x_i - B \geq 0, \quad (22)$$

is replaced by a penalization term in the QUBO formulation that makes larger penalization for negative terms and smaller for positive. The idea of the unbalanced penalization function comes from the shape of the exponential decay curve,  $f(x) = e^{-h(x)}$ . In this function, positive values of  $h(x)$ , Eq. (22) make  $f(x) \approx 0$  while negative values make it grow exponentially, as it is shown in Fig. 3. However, the exponential function cannot be encoded as a QUBO penalization term. Therefore, we consider an

expansion of the exponential function to quadratic order. In such a case, the penalization term is given by

$$e^{-h(x)} \approx 1 - h(x) + \frac{1}{2}h(x)^2. \quad (23)$$

In general, we modify Eq. (23) to include free parameters to be adjusted for the different kinds of problems. Therefore, Eq. (23) is rewritten by

$$\zeta(x) = \lambda_2 h(x)^2 - \lambda_1 h(x) \quad (24)$$

$$= \lambda_2 \left( \sum_i l_i x_i - B \right)^2 - \lambda_1 \left( \sum_i l_i x_i - B \right) \quad (25)$$

where  $\lambda_{1,2}$  are a set of multipliers that can be tuned for the specific problem and the constant term is removed because the position of the cost function's minimum is independent of the constant term. The new cost function based on Eq. (9) and the unbalanced penalization approach is given by

$$\min_x \left( \sum_{i=1}^n \sum_{j \neq i}^n c_{ij} x_i x_j + \sum_{i=1}^n h_i x_i + \lambda_0 \left( \sum_{i=1}^n q_i x_i - C \right)^2 + \lambda_2 \left( \sum_i l_i x_i - B \right)^2 - \lambda_1 \left( \sum_i l_i x_i - B \right) \right), \quad (26)$$

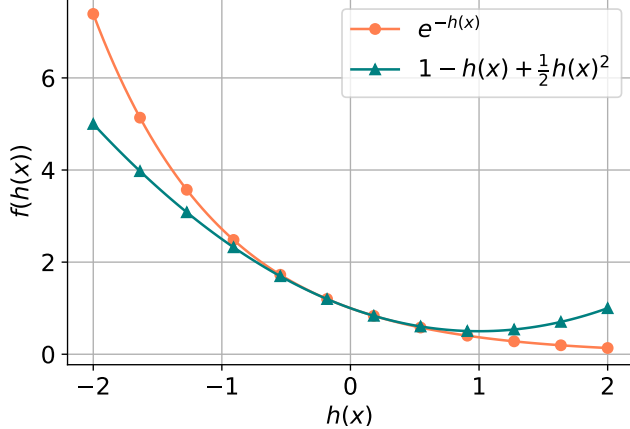


FIG. 3. Comparison between  $e^{-h(x)}$  and the unbalanced function  $1 - h(x) + \frac{1}{2}h(x)^2$ .

To tune the  $\lambda_{0,1,2}$  parameters of Eq. (26) for the TSP, the BPP, and the KP, we use the Nelder-Mead optimization method to explore the set of  $\lambda_{0,1,2}$  values that brings the optimal solution as close as possible to the ground state of the cost Hamiltonian, Eq. (10.) For the case of the TSP, we use a random problem with 4 cities, for the BPP we use a random problem with 4 items, and for the KP we use a problem with 13 items. The set of values  $\lambda_{0,1,2}$  found using the method mention before for each problem are presented in Table I. After we find the best

set of values for the specific problem, we test if those values generalize to other random cases. This is a crucial aspect of the unbalanced penalization method that the set of  $\lambda_{0,1,2}$  of a random case generalizes for different and/or larger problems. The results about these aspects of the unbalanced penalization method are presented in Sec. IV.

TABLE I. Summary of the parameters  $\lambda_{0,1,2}$  for the TSP, BPP, and KP used to translate the combinatorial optimization problems into the QUBO representation using the unbalanced penalization approach (Eq. (26).)

	$\lambda_0$	$\lambda_1$	$\lambda_2$
TSP	38.2584	18.2838	57.0375
BPP	20.5198	7.2949	0.8583
KP	1.0792	0.9603	0.0371

### Quantum Approximate Optimization Algorithm

Finally, to test the difference between the slack variables approach vs. the unbalance penalization encoding on different random problems of the TSP, the BPP, and the KP, we use the QAOA with one layer. In this case, the cost Hamiltonian ( $H_c$ ), obtained from the QUBO formulation, is translated into a parametric unitary gate

given by

$$U(H_c, \gamma) = e^{-i\gamma H_c} \quad (27)$$

where  $\gamma$  is a parameter to be optimized. A second unitary operator applied is

$$U(B, \beta) = e^{i\beta B} \quad (28)$$

where  $\beta$  is the second parameter that must be optimized and  $B = \sum_{i=1}^n \sigma_i^x$  with  $\sigma_i^x$  the Pauli-x quantum gate applied to qubit  $i$ . The general QAOA circuit is shown in Fig. 4; here,  $R_X(\theta) = e^{-i\frac{\theta}{2}\sigma_x}$ ,  $p$  represents the number of repetitions of the unitary gates of Eqs. 27 and 28 with each repetition having separate values for  $\gamma_p$  and  $\beta_p$  values, and the initial state is a superposition state  $|+\rangle^{\otimes n}$ . The case of QAOA with  $p=1$  is suitable for visualization of the landscape and in Sec. IV, we show a comparison between both encodings and even though they are similar, the addition of extra qubits for the slack variables approach has a great impact on the probability of finding the optimal solution.

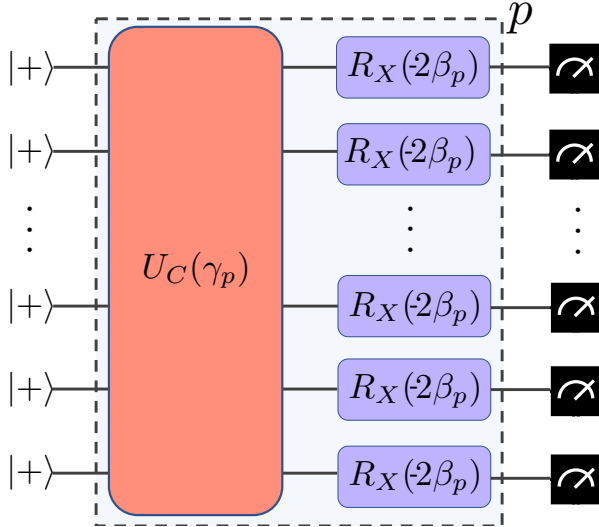


FIG. 4. Schematic representation of QAOA for  $p$  layers. The parameter  $\gamma$  and  $\beta$  for each layer are the ones to be optimized. QAOA is used to compare the slack approach vs. the unbalanced one for the encoding of the inequality constraints.

#### Coefficient of performance

Additionally, we introduce the coefficient of performance (CoP), a quantifier that expresses how good a solution is compared to random guessing over a set of solutions. In this perspective, we use the CoP to determine how likely it is to find the optimal solution for the TSP, the BPP, and the KP on the local minima of the QAOA algorithm for  $p = 1$ . The CoP is given by

$$CoP = \frac{P(*x)}{P_R}, \quad (29)$$

where  $P(*x)$  is the probability of getting a bit string  $*x$  using a quantum algorithm, e.g., QAOA and  $P_R = 1/2^n$  is the probability of a random guessing with  $n$  equal to the number of qubits involved in the problem.

## IV. RESULTS

### Optimal Solution distribution

To determine the applicability of our method, we sorted the eigenvalues of the cost Hamiltonian for the different combinatorial optimization problems. The parameter of interest is the position of the eigenvalue that describes the optimal solution within the list of all sorted eigenvalues of the cost Hamiltonian. If the position of the optimal solution is far from the ground energy of the cost Hamiltonian, the unbalanced penalization encoding is not working as expected. Otherwise, if the optimal solution is close to the ground energy given the total number of eigenvalues, the unbalanced encoding is advantageous.

Figure 5 shows the eigenvalues of 10 random cases for the 5 nodes TSP using the unbalanced penalization encoding approach. In this case, the eigenvalues are sorted in terms of their energy from the minimum to the maximum with the x-axis representing the eigenvalue position, and the y-axis its energy. In the inset, the big circles represent where the optimal result is compared to all the other eigenvalues (small circles) of the cost Hamiltonian. Here, the worst eigenvalue position is 6 out of 1048576 eigenvalues ( $2^{20}$ ), this means that in the worst scenario the optimal solution is among the lowest 0.00057% of all eigenvalues.

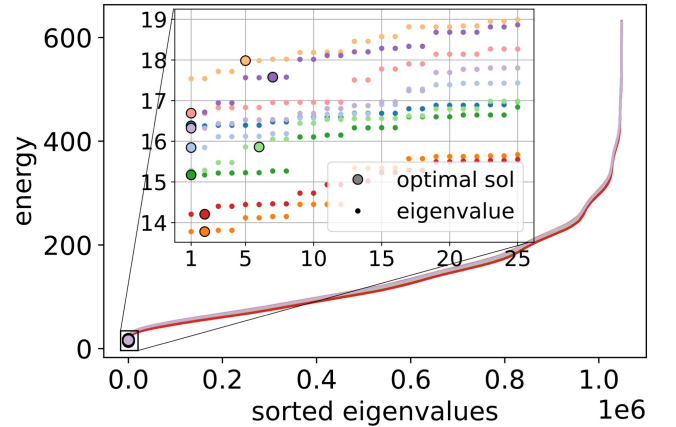


FIG. 5. Eigenvalues distribution for the TSP with 5 cities (20 qubits) for 10 randomly generated problems using the unbalanced penalization method. The big circles are the optimal solutions for the random problem and the small circles are the different eigenvalues, note that each eigenenergy is degenerate with multiplicity two, this is because the problem is symmetric, e.g., one solution clockwise and other anti-clockwise.

In this new scenario, the unbalanced penalization approach does not ensure that the optimal solution is the lowest eigenvalue of the cost Hamiltonian, but in all the cases analyzed, it is very close to it. For example, in Fig. 6, this feature is illustrated for one of the random problems of Fig. 5. Here, there are a couple of eigenvalues that do not fulfill all the restrictions of the problem but have lower energy than the optimal solution. In the end, the unbalanced penalization encoding is a trade-off between adding slack variables and ensuring the ground state is the optimal solution or reduce the number of variables but encoding the optimal solution in the vicinity of the ground state. In many cases, there is no preference for encoding the optimal solution in the lowest eigenvalue. For instance, QAOA brings the expectation value of a cost Hamiltonian to a region of overall minimum energy, so we can expect that the optimal and suboptimal solutions occur with reasonable probability in regions of minimal energy.

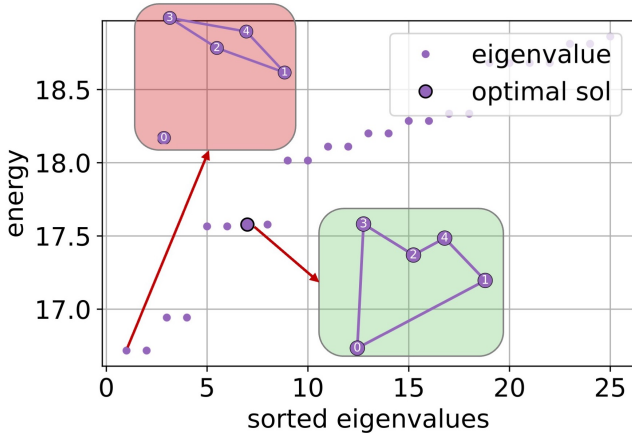


FIG. 6. The first 25 sorted eigenvalues of the Hamiltonian  $H_c$  corresponding to the worst case in Fig. 5. The big circle corresponds to the optimal solution to this problem and the small circles are the other eigenvalues. The solution in the red inset is the ground state which is not a valid solution, while the solution in the green inset is the optimal solution.

Fig. 7 shows the energy of the different eigenvalues sorted for the cost Hamiltonian of the BPP for 10 random problems with 5 items. In the inset, the optimal solutions are highlighted with big circles and the small circles are the other eigenvalues. In this case, there is an increasing number of degeneracies explained by the symmetries of the problem (interchange the items from of one bin with the others). To keep the same number of qubits (21) for all the problems, we select 10 random cases that require more than 3 bins to store the items. Here, the worst case is in the position 36 out of 2097152 eigenvalues ( $2^{21}$ ) which means it is within 0.00124%, of all eigenvalues.

Finally, Fig. 8 shows the eigenvalues distribution for 10 random cases of the KP with 21 items (21 qubits). In this case, there are no degeneracies, but the possible solutions are close to each other. The inset shows the

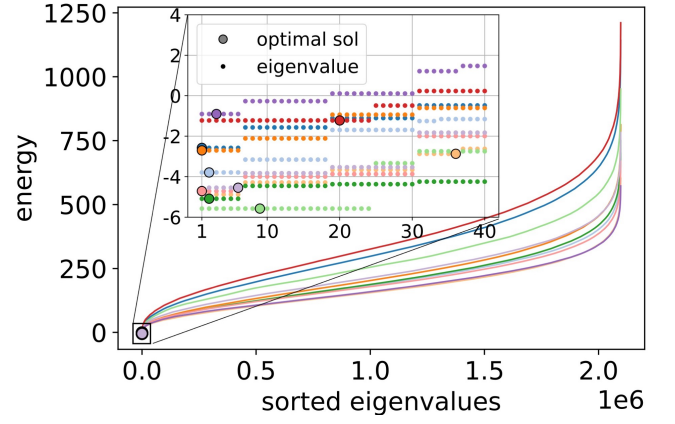


FIG. 7. Eigenvalues distribution for the BPP with 5 items (21 qubits) for 10 randomly generated problems using the unbalanced inequality-constrained penalization method. The big points are the optimal solutions for the random problem and the small points are the different eigenvalues. Note that each eigenenergy has a different number of degeneracies, this is because the problem has some symmetries.

first 50 eigenvalues, in this case one of the random cases has the optimal solution in the position 49 out of 2097152 eigenvalues ( $2^{21}$ ) which means it is within 0.0023% of the first eigenvalues. In this case, the parameters  $\lambda_{0,1,2}$  were optimized for a 13 items random case, which suggests great generalization capabilities of the current method.

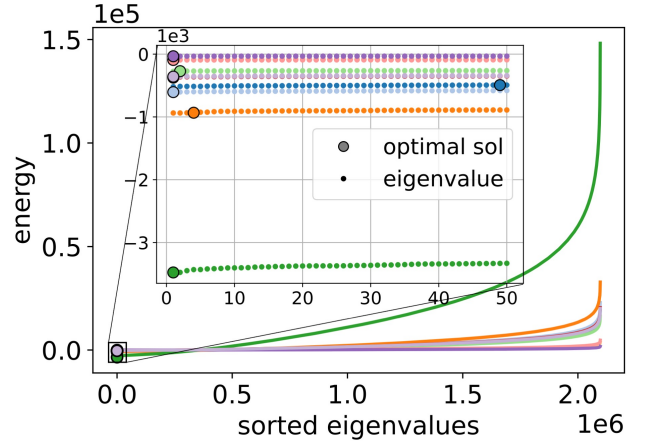


FIG. 8. Eigenvalues distribution for the KP with 21 items (21 qubits) for 10 randomly generated problems using the unbalanced penalization method. The big circles are the optimal solutions for the random problem and the small circles are the different eigenvalues. In this case, there are no degeneracies but the energies are close to each other.

### QAOA landscape

The results of the cost Hamiltonian landscape using the QAOA algorithm with one layer is presented in this



section for the TSP, the BPP, and the KP. The slack variables method and the unbalanced penalization method are used for the cost Hamiltonian encoding. For visualization purposes, the landscape in all the cases is limited to the region of  $\gamma \in (-\pi/\max\{q_{ij}\}, 0)$  where  $q_{ij}$  is given in Eq. (10.) This is because a specific region enables a direct comparison of the landscapes and the probability of the optimal solution.

Fig. 9 shows the energy landscape of the QAOA algorithm for a TSP with 4 cities; this is equivalent to 17 and 12 qubits for the slack variables and the unbalanced penalization encodings, respectively. The probabilities of finding the optimal solutions are 0.02% and 0.227% for the slack variables and the unbalanced encodings, respectively. This shows a clear advantage of the unbalanced encoding method increasing the probability more than 10 times with respect to the probability of the slack variables encoding. This characteristic is mainly attributed to the difference in number of qubits needed to represent the problem and therefore the set of possible solutions, for the slack variables there are 131072 ( $2^{17}$ ) possible solutions while for the unbalanced penalization there are 4096 ( $2^{12}$ ) possible solutions.

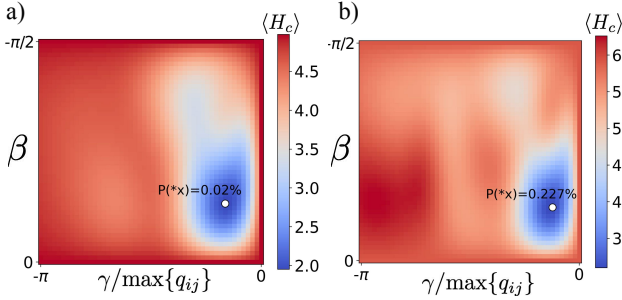


FIG. 9. Cost Hamiltonian  $\langle H_c \rangle$  expectation value landscape comparison between a) slack encoding and b) unbalanced penalization encoding for a 4 cities TSP. The cost function minimum value is shown with a white dot and the optimal solution probability in this point. Both results are for the QAOA with 1 layer.

Fig. 10 shows the energy landscape of the QAOA algorithm for a BPP with 3 items which is equivalent to 6 and 19 qubits for the unbalanced and slack encodings, respectively. The probability of finding the optimal solution in the local minima of QAOA is 0.001% for the slack variables encoding and 10.66% for the unbalance penalization method. Here, the optimal solution is 10000 times more likely to be found using the unbalanced penalization approach than using the slack variables approach.

Finally, Fig. 11 shows the energy landscape of the QAOA algorithm for a knapsack problem with 10 items which is equivalent to 18 and 10 qubits for the slack variables and the unbalanced penalization encoding, respectively. Here, the probability to find the optimal solution is 0.001% and 0.346% for the slack variables and the unbalanced penalization encoding. This means finding the

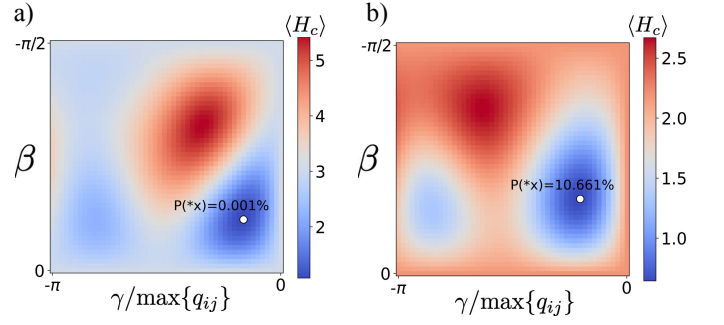


FIG. 10. Cost Hamiltonian  $\langle H_c \rangle$  expectation value landscape comparison between a) slack encoding and b) unbalanced penalization encoding for a 3 items BPP. The cost function minimum value is shown with a white dot and the optimal solution probability in this point. Both results are for the QAOA with 1 layer.

solution with the unbalanced penalization method is 346 times more likely than with the slack variables encoding.

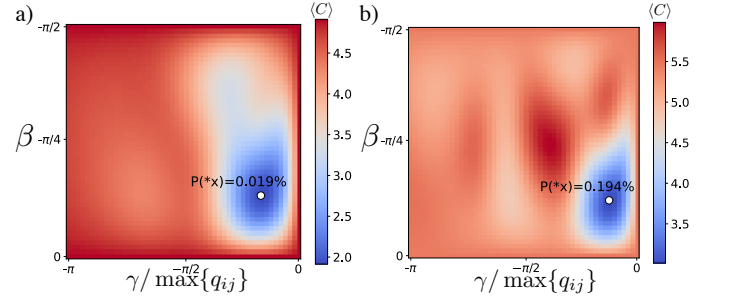


FIG. 11. Cost function landscape  $\langle C \rangle$  comparison between a) slack encoding and b) unbalanced penalization encoding for a 10 items KP. The cost function minimum value is shown with a white dot and the optimal solution probability in this point. Both results are for the QAOA with 1 layer.

### The coefficient of performance

Figure 12 shows the CoP for different problem sizes for the TSP, BPP, and KP using the unbalanced penalization method. All the cases show the probability of the optimal solution for each problem using QAOA with 1 layer in the minimum point of the energy landscape region  $\beta \in (-\pi/2, 0)$  and  $\gamma \in (-\pi/\max\{q_{ij}\}, 0)$ . At this point, we do not use a classical optimizer to find the optimal beta and gamma, but instead, we divide the beta and gamma region by a 50x50 grid landscape and take the probability of the optimal solution at the minimum energy. It is expected that using an optimization method for this step improves the CoP while keeping the same tendency. Fig. 12 a) shows the CoP for the TSP problem for cities 2, 3, 4, 5, 6, and 7 (2, 6, 12, 20, 30, and 42 qubits). For the cases with 30 and 42 qubits, we use the Jülich universal quantum computer simulator (JUQCS)



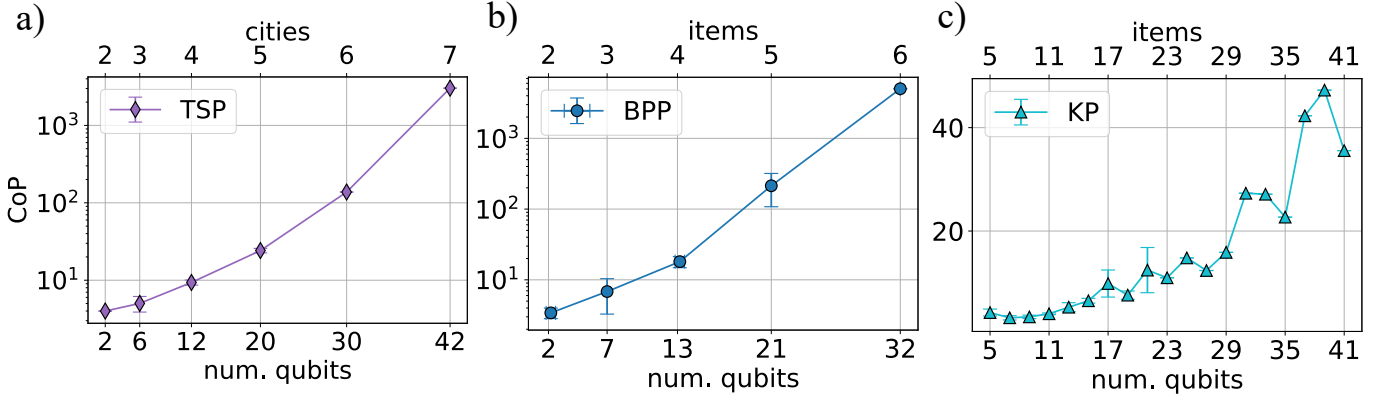


FIG. 12. Coefficient of performance for a) the TSP, b) the BPP, and c) the KP for different problem size. The points of the TSP correspond to 2, 3, 4, 5, 6, and 7 cities. The points of the BPP corresponds to 2, 3, 4, 5, and 6 items. Finally, the KP points correspond to 5 to 41 items with increments of 2. The error bars represent the standard deviation over 5 different random cases for problems below 22 qubits. For problems with more than 21 qubits the points represent 1 case.

[32, 33] in its GPU-accelerated version [34]. The simulations with 42 qubits were performed on JUWELS Booster [35] as they require more than 1/16 PiB of distributed GPU memory. Note that the same TSP cases using the slack variables approach will require 2, 7, 17, 36, 73, 148, and 304 qubits. Therefore, we are exploring problem size (5, 6, and 7 cities) unfeasible using the slack approach on quantum computer simulators. Interestingly, the CoP is increasing exponentially with the problem size, which means that finding the optimal solution exponentially increases when we compare it with a random guessing in the set of possible configurations (cf. [36]).

Fig. 12 b) shows the CoP for the BPP for 2, 3, 4, 5, and 6 items (2, 6, 13, 21, and 32 qubits). For this case, the CoP is improving even more rapidly compared to TSP and again for the 6 items, case the solution using slack variables (61 qubits) is out of what can be simulated with quantum computer simulators. Finally, Fig. 12 c) shows the CoP for the Knapsack problem for 5 to 41 items with increments of two (same number of qubits), in this case, the CoP increase linearly with the number of qubits. This is a poor performance if we compare it with the TSP and BPP, and we suspect the improved CoP is related to the number of constraints of the problem.

## V. CONCLUSIONS

We have presented *unbalanced penalization*, a new method to encode inequality constraints of combinatorial optimization problems into QUBO penalizations. The method does not require extra slack variables to encode the inequality constraints. This is extremely beneficial because there is no increase in the number of variables or qubits needed to encode the problems, especially for the TSP and the BPP.

The method is suited for quantum annealing or VQA where encoding the QUBO of combinatorial optimization

problems is needed. We have tested the method using QAOA with 1 layer on the TSP, BPP, and KP and we show that in 10 random cases for different problem sizes the optimal solution is located in the vicinity of the ground state of the cost Hamiltonian  $H_c$ . The method is highly generalizable in the sense that the tuned parameters  $\lambda_{0,1,2}$  for small problems generalize well to larger cases. Additionally, the probabilities to find the optimal solutions in the local minima of the unbalanced penalization (Figs. 9 to 11) are much better than using slack variables. Qualitatively, this can be understood because the addition of slack variables increases the search space and therefore reduces the probability of finding optimal and sub-optimal solutions.

We have tested the unbalanced penalization method close to the limits of what is possible to be simulated on supercomputers using JUQCS. For the case of TSP, we went up to 42 qubits, for BPP up to 32 qubits, and for KP up to 41 qubits. Indeed, we are exploring regions unfeasible using the slack approach. For example, the case of the TSP with 6 and 7 cities using the slack approach requires 73 and 148 qubits, and the BPP with 6 items requires 61 qubits. In terms of probability, the unbalanced penalization approach shows large advantages in the small cases we compare. For the TSP with 4 cities, the optimal solution probability at the local minimum energy using the unbalanced penalization method is more than 10 times greater than using the slack variables approach. For the BPP with 3 items, the improvement in probability is more than 10000 times greater, and for the KP with 10 items the improvement is almost 346.

Finally, we have presented a new metric, the CoP, which is useful to compare the probability of a specific solution (in this case the optimal solution) against random guessing. We have shown the CoP for the TSP, the BPP, and the KP using QAOA with  $p=1$  in the region  $\gamma \in (-\pi/\max\{q_{ij}\}, 0)$  and  $\beta \in (-\pi/2, 0)$ . Interestingly, for all of them, the CoP increases with the size of the

problem, for the KP problem increases linearly while for the TSP and BPP the increase is exponential. Further search in this direction is needed to see if this provides an implicit advantage of using QAOA to solve combinatorial optimization problems, what are the characteristics of the TSP and the BPP that make the CoP increase exponentially, and how increasing the number of QAOA layers improves the CoP.

## ACKNOWLEDGMENTS

We would like to thank Leonardo Disilvestro and Vishal Sharma from Entropica Labs for helpful comments

and suggestions about the results of the present work.

J. A. Montañez-Barrera acknowledges support by the German Federal Ministry of Education and Research (BMBF), funding program Quantum technologies - from basic research to market, project QSolid (Grant No. 13N16149). D.W. acknowledges support from the project Jülich UNified Infrastructure for Quantum computing (JUNIQ) that has received funding from the German Federal Ministry of Education and Research (BMBF) and the Ministry of Culture and Science of the State of North Rhine-Westphalia. The authors gratefully acknowledge the Gauss Centre for Supercomputing e.V. ([www.gauss-centre.eu](http://www.gauss-centre.eu)) for funding this project by providing computing time on the GCS Supercomputer JUWELS at Jülich Supercomputing Centre (JSC).

- 
- [1] A. Lucas, “Ising formulations of many NP problems,” *Frontiers in Physics*, vol. 2, pp. 1–14, 2014.
  - [2] G. Kochenberger, J. K. Hao, F. Glover, M. Lewis, Z. Lü, H. Wang, and Y. Wang, “The unconstrained binary quadratic programming problem: A survey,” *Journal of Combinatorial Optimization*, vol. 28, no. 1, pp. 58–81, 2014.
  - [3] M. Ohzeki, “Breaking limitation of quantum annealer in solving optimization problems under constraints,” *Scientific Reports*, vol. 10, no. 1, pp. 1–12, 2020.
  - [4] M. P. Harrigan, K. J. Sung, M. Neeley, K. J. Satzinger, F. Arute, K. Arya, J. Atalaya, J. C. Bardin, R. Barends, S. Boixo, M. Broughton, B. B. Buckley, D. A. Buell, B. Burkett, N. Bushnell, Y. Chen, Z. Chen, Ben Chiaro, R. Collins, W. Courtney, S. Demura, A. Dunsworth, D. Eppens, A. Fowler, B. Foxen, C. Gidney, M. Giustina, R. Graff, S. Habegger, A. Ho, S. Hong, T. Huang, L. B. Ioffe, S. V. Isakov, E. Jeffrey, Z. Jiang, C. Jones, D. Kafri, K. Kechedzhi, J. Kelly, S. Kim, P. V. Klimov, A. N. Korotkov, F. Kostritsa, D. Landhuis, P. Laptev, M. Lindmark, M. Leib, O. Martin, J. M. Martinis, J. R. McClean, M. McEwen, A. Megrant, X. Mi, M. Mohseni, W. Mruczkiewicz, J. Mutus, O. Naaman, C. Neill, F. Neukart, M. Y. Niu, T. E. O’Brien, B. O’Gorman, E. Ostby, A. Petukhov, H. Putterman, C. Quintana, P. Roushan, N. C. Rubin, D. Sank, A. Skolik, V. Smelyanskiy, D. Strain, M. Streif, M. Szalay, A. Vainsencher, T. White, Z. J. Yao, P. Yeh, A. Zalcman, L. Zhou, H. Neven, D. Bacon, E. Lucero, E. Farhi, and R. Babbush, “Quantum approximate optimization of non-planar graph problems on a planar superconducting processor,” *Nature Physics*, vol. 17, no. 3, pp. 332–336, 2021.
  - [5] P. Niroula, R. Shaydulin, R. Yalovetzky, P. Minssen, D. Herman, S. Hu, and M. Pistoia, “Constrained Quantum Optimization for Extractive Summarization on a Trapped-ion Quantum Computer,” 2022.
  - [6] J. Preskill, “Quantum computing in the NISQ era and beyond,” *Quantum*, vol. 2, no. July, pp. 1–20, 2018.
  - [7] P. W. Shor, “Algorithms for quantum computation: discrete logarithms and factoring,” in *Proceedings 35th Annual Symposium on Foundations of Computer Science*, pp. 124–134, Nov 1994.
  - [8] P. W. Shor, “Polynomial-time algorithms for prime factorization and discrete logarithms on a quantum computer,” *SIAM J. Comput.*, vol. 26, no. 5, pp. 1484–1509, 1997.
  - [9] M. Cerezo, A. Arrasmith, R. Babbush, S. Benjamin, S. Endo, K. Fujii, J. McClean, K. Mitarai, X. Yuan, L. Cincio, and P. Coles, “Variational quantum algorithms,” *Nature Reviews Physics*, vol. 3, pp. 1–20, 08 2021.
  - [10] S. Khairy, R. Shaydulin, L. Cincio, Y. Alexeev, and P. Balaprakash, “Learning to optimize variational quantum circuits to solve combinatorial problems,” *Proceedings of the AAAI Conference on Artificial Intelligence*, vol. 34, pp. 2367–2375, 04 2020.
  - [11] D. de Falco and D. Tamascelli, “An introduction to quantum annealing,” *RAIRO - Theoretical Informatics and Applications*, vol. 45, 07 2011.
  - [12] R. Ayanzadeh, J. Dorband, M. Halem, and T. Finin, “Multi-qubit correction for quantum annealers,” *Scientific Reports*, vol. 11, no. 1, pp. 1–12, 2021.
  - [13] B. Heim, T. F. Rønnow, S. V. Isakov, and M. Troyer, “Quantum versus classical annealing of Ising spin glasses,” *Science*, vol. 348, no. 6231, pp. 215–217, 2015.
  - [14] B. Yan and N. A. Sinitsyn, “Analytical solution for nonadiabatic quantum annealing to arbitrary Ising spin Hamiltonian,” *Nature Communications*, vol. 13, no. 1, pp. 1–15, 2022.
  - [15] B. Tasseff, T. Albash, Z. Morrell, M. Vuffray, A. Y. Lokhov, S. Misra, and C. Coffrin, “On the Emerging Potential of Quantum Annealing Hardware for Combinatorial Optimization,” pp. 1–25, 2022.
  - [16] E. Farhi, J. Goldstone, and S. Gutmann, “A quantum approximate optimization algorithm,” 11 2014.
  - [17] H. Jiang, Z.-J. M. Shen, and J. Liu, “Quantum Computing Methods for Supply Chain Management,” 2022.
  - [18] R. Orús, S. Mugel, and E. Lizaso, “Quantum computing for finance: Overview and prospects,” *Reviews in Physics*, vol. 4, pp. 1–13, 2019.
  - [19] A. M. Souza, E. O. Martins, I. Roditi, N. Sá, R. S. Sarthour, and I. S. Oliveira, “An Application of Quantum Annealing Computing to Seismic Inversion,” *Frontiers in Physics*, vol. 9, no. January, pp. 1–8, 2022.
  - [20] S. Mugel, C. Kuchkovsky, E. Sánchez, S. Fernández-

- Lorenzo, J. Luis-Hita, E. Lizaso, and R. Orús, “Dynamic portfolio optimization with real datasets using quantum processors and quantum-inspired tensor networks,” *Physical Review Research*, vol. 4, no. 1, pp. 1–13, 2022.
- [21] M. T. A. Sharabiani, V. B. Jakobsen, M. Jeppesen, and A. S. Mahani, “Quantum Computing in Green Energy Production,” pp. 1–35, 2021.
- [22] H. Urgelles, P. Picazo-martinez, D. Garcia-roger, and J. F. Monserrat, “Multi-Objective Routing Optimization for 6G Communication Networks Using a Quantum Approximate Optimization Algorithm,” 2022.
- [23] A. Luckow, J. Klepsch, and J. Pichlmeier, “Quantum Computing: Towards Industry Reference Problems,” *Digitale Welt*, vol. 5, no. 2, pp. 38–45, 2021.
- [24] D. Inoue, A. Okada, T. Matsumori, K. Aihara, and H. Yoshida, “Traffic signal optimization on a square lattice with quantum annealing,” *Scientific Reports*, vol. 11, no. 1, pp. 1–14, 2021.
- [25] V. Sharma, N. S. B. Saharan, S.-H. Chiew, E. I. R. Chiachio, L. Disilvestro, T. F. Demarie, and E. Munro, “OpenQAOA – An SDK for QAOA,” pp. 1–10, 2022.
- [26] F. Glover, G. Kochenberger, and Y. Du, “Quantum Bridge Analytics I: a tutorial on formulating and using QUBO models,” *4or*, vol. 17, no. 4, pp. 335–371, 2019.
- [27] “Penalty and partitioning techniques to improve performance of QUBO solvers,” *Discrete Optimization*, vol. 44, no. xxxx, p. 100594, 2022.
- [28] M. Grötschel and G. L. Nemhauser, “George Dantzig’s contributions to integer programming,” *Discrete Optimization*, vol. 5, no. 2, pp. 168–173, 2008.
- [29] K. Heßler, S. Irnich, T. Kreiter, and U. Pferschy, “Lexicographic Bin-Packing Optimization for Loading Trucks in a Direct-Shipping System,” no. 2009, 2020.
- [30] J. Yan, Y. Lu, L. Chen, S. Qin, Y. Fang, Q. Lin, T. Mosciro, S. Rajmohan, and D. Zhang, *Solving the Batch Stochastic Bin Packing Problem in Cloud: A Chance-constrained Optimization Approach*, vol. 1. Association for Computing Machinery, 2022.
- [31] M. Kroes, L. Petrica, S. Cotozana, and M. Blott, “Evolutionary bin packing for memory-efficient dataflow inference acceleration on FPGA,” *GECCO 2020 - Proceedings of the 2020 Genetic and Evolutionary Computation Conference*, pp. 1125–1133, 2020.
- [32] K. De Raedt, K. Michielsen, H. De Raedt, B. Trieu, G. Arnold, M. Richter, Th. Lippert, H. Watanabe, and N. Ito, “Massively parallel quantum computer simulator,” *Comput. Phys. Commun.*, vol. 176, no. 2, p. 121, 2007.
- [33] H. De Raedt, F. Jin, D. Willsch, M. Willsch, N. Yoshioka, N. Ito, S. Yuan, and K. Michielsen, “Massively parallel quantum computer simulator, eleven years later,” *Comput. Phys. Commun.*, vol. 237, pp. 47 – 61, 2019.
- [34] D. Willsch, M. Willsch, F. Jin, K. Michielsen, and H. De Raedt, “GPU-accelerated simulations of quantum annealing and the quantum approximate optimization algorithm,” *Comput. Phys. Commun.*, vol. 278, p. 108411, 2022.
- [35] S. Kesselheim, A. Herten, K. Krajsek, J. Ebert, J. Jitsev, M. Cherti, M. Langguth, B. Gong, S. Stadtler, A. Mozafari, G. Cavallaro, R. Sedona, A. Schug, A. Strube, R. Kamath, M. G. Schultz, M. Riedel, and Th. Lippert, “JUWELS Booster – A Supercomputer for Large-Scale AI Research.” 2021.
- [36] D. Willsch, M. Jattana, M. Willsch, S. Schulz, F. Jin, H. De Raedt, and K. Michielsen, “Hybrid Quantum Classical Simulations,” in *NIC Symposium 2022* (M. Müller, C. Peter, and A. Trautmann, eds.), vol. 51 of *Publication Series of the John von Neumann Institute for Computing (NIC) NIC Series*, (Jülich), pp. 31–44, Forschungszentrum Jülich GmbH Zentralbibliothek, Verlag.